

HeadLighter: Disentangling Illumination in Generative 3D Gaussian Heads via Lightstage Captures

Yating Wang^{1†} Yuan Sun^{2†} Xuan Wang² Ran Yi^{1*} Boyao Zhou² Yipengjing Sun²
 Hongyu Liu² YINUO Wang² Lizhuang Ma^{1*}
¹Shanghai Jiao Tong University ²AntGroup Research

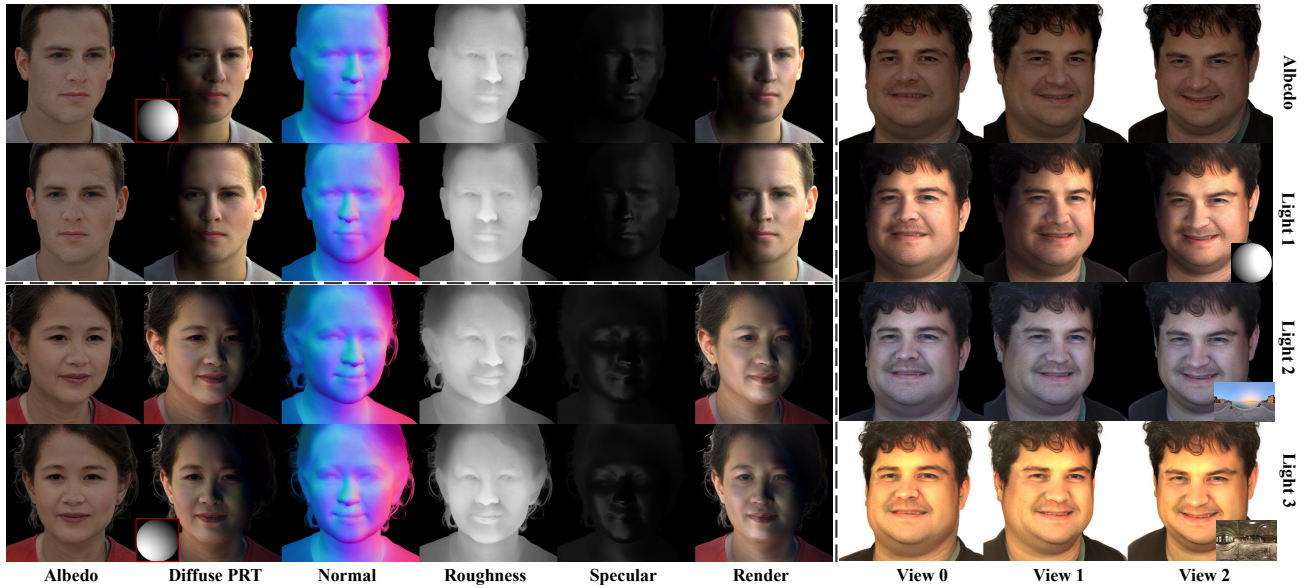


Figure 1. Our method achieves high-fidelity disentanglement of intrinsic appearance and illumination in generative 3D Gaussian head models. It produces photorealistic intrinsic attributes including albedo, normals, and roughness, and supports relighting under diverse lighting conditions such as environment maps, spherical harmonics, and point lights. Left: intrinsic appearance attributes of two generated subjects. Right: relighting results of one subject under varying illumination.

Abstract

Recent 3D-aware head generative models based on 3D Gaussian Splatting achieve real-time, photorealistic and view-consistent head synthesis. However, a fundamental limitation persists: the deep entanglement of illumination and intrinsic appearance prevents controllable relighting. Existing disentanglement methods rely on strong assumptions to enable weakly supervised learning, which restricts their capacity for complex illumination. To address this challenge, we introduce *HeadLighter*, a novel supervised framework that learns a physically plausible decomposition of appearance and illumination in head generative models. Specifically, we design a dual-branch architecture that separately models lighting-invariant head attributes and physically grounded rendering components. A progressive disentanglement training is employed to gradually inject head

appearance priors into the generative architecture, supervised by multi-view images captured under controlled light conditions with a light stage setup. We further introduce a distillation strategy to generate high-quality normals for realistic rendering. Experiments demonstrate that our method preserves high-quality generation and real-time rendering, while simultaneously supporting explicit lighting and view-point editing. We will publicly release our code and dataset.

1. Introduction

Generative models for 3D human heads have seen remarkable progress, driven by their wide-ranging applications in digital avatars, virtual reality, and the entertainment industry. Among them, the most prominent approaches are 3D-aware Generative Adversarial Networks (GANs) built upon neural rendering techniques [22, 27]. These models learn

a rich prior of 3D head geometry and appearance directly from large-scale 2D in-the-wild images, without requiring any explicit 3D supervision. Consequently, they can synthesize highly realistic and view-consistent 3D head with rich identity and appearance diversity. In the pursuit of real-time performance and impressive visual quality, recent works integrate 3D Gaussian Splatting (3DGS) into the generative framework [2, 23], replacing the computationally intensive volume rendering and achieving real-time rendering.

However, a critical limitation persists: the illumination and the intrinsic head appearance (i.e., material or albedo) are deeply entangled, fundamentally preventing fine-grained control over the lighting conditions of the generated 3D heads. Existing approaches enable unsupervised decomposition of pretrained generative models using simplified reflectance models or strong assumptions. NFL [18] involve style-mixing supervision with the white-light and face symmetry assumption, initializing from a on-the-shell light estimator, while GSHR [24] introduce a simplified light transport function for 3D gaussian and distill albedo and shading from NFL [18]. Others [12, 32] enforce physically plausible shading in neural volume rendering to split the diffuse and specular components. While these methods support explicit lighting control, their lack of real-world data limits their ability to handle complex lighting and achieve high physical plausibility.

We address this by an intuitive and straight forward way: involving a multi-view face dataset captured under controlled illuminations with a LightStage to learn this disentanglement. However, directly utilizing this dataset is non-trivial: compared to large-scale in-the-wild face image datasets, our light stage dataset covers only a limited range of identities and lighting conditions, and exhibits a noticeable domain gap relative to natural imagery. To prevent overfitting on the light stage dataset and to preserve the generalization capability of the base generative model, we decompose pretrained generative model into a dual-branch architecture: **1)** a light-invariant base branch to generate geometry and albedo of 3D gaussian, and **2)** a relight branch predicting attributes for physically-based rendering. And we further design a progressive training schema to ensure stable disentanglement. Firstly a pretrained generative model is shifted into light-invariant domain as the base branch to preserve rich generative prior of human heads. Guided by frozen base branch, we inject face appearance priors embedded in lightstage captures into the relight branch. Finally, two branches are trained jointly for better generalization.

A further challenge lies in obtaining accurate surface normals, which are crucial for realistic shading but not native to 3D gaussian representations. While computing normals from extracted mesh or neighbor splats are feasible, such methods are computationally expensive in training it-

erations and can introduce significant noise. Observing that the base branch encodes gaussian geometry, we task the relight branch to directly predict plausible normals guided by base branch features. We further introduce a distillation strategy and smoothness terms that enforce consistent and plausible normal prediction, enabling photorealistic rendering of complex shading effects.

We demonstrate the effectiveness of our pipeline through comprehensive comparisons with state-of-the-art methods. We evaluate generative diversity, rendering speed and multi-view spatial consistency of our disentangled generative models. We demonstrate the rendering results of 3D human heads generated by our method under different lighting inputs. To further validate the disentanglement capability, we quantitatively and qualitatively compare free-view relighting performance by extracting image pairs with varying poses and lighting conditions from our real-captured dataset. To foster future research, we will make our code and licensed dataset publicly available.

2. Related Works

2.1. 3D-aware Generative Head Models

The pursuit of high-fidelity, view-consistent, and controllable 3D human head synthesis has led to the rapid evolution of 3D-aware Generative Adversarial Networks. These models learn to generate 3D heads from large-scale 2D image sets, bypassing the need for large-scale 3D supervision. Early 3D GANs leverage various 3D representations [7, 8, 37, 40, 42] into the GAN framework. Among them, EG3D [8] proposes a hybrid tri-planes, achieving photorealistic visual quality. But its reliance on volume rendering is computationally expensive, and super-resolution modules introduce view inconsistencies. To facilitate efficient, high-resolution generative head models, recent methods like [2, 23, 48] have turned to 3D Gaussian Splatting (3DGS) [22]. However, a fundamental limitation is that intrinsic face appearance properties and lighting are conflated into a view-dependent color, which makes direct and physically-plausible relighting impossible.

To enable explicit lighting control, a line of research [12, 18, 19, 24, 28, 32, 41] has focused on disentangling illumination. NFL [18] distills pseudo albedo and shading from pretrained EG3D [8] model by style-mixing, constrained by white-light, face symmetry assumption and an on-the shell light estimator. LumiGAN [12] and FaceLit [32] employ an inverse rendering framework to separately model diffuse and specular components. GSHR [24] achieves highly efficient synthesis by designing a simplified radiance transfer representation for 3D Gaussians, but it relies on supervision from the pseudo-data generated by NFL [18]. Ultimately, these approaches lack access to ground-truth data, so they must resort to strong, simplifying assumptions that

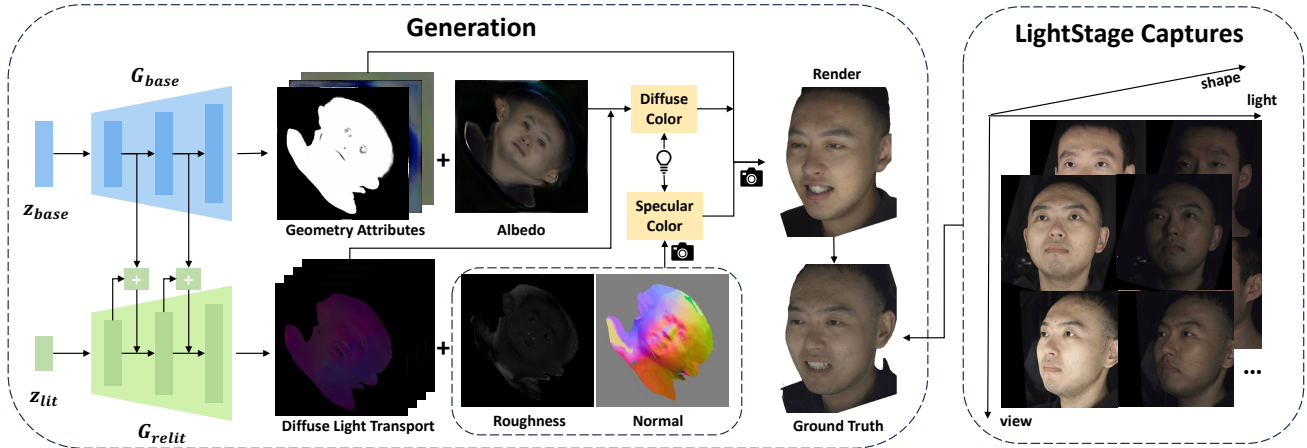


Figure 2. **Our proposed framework.** We leverage real-world captures to learn high-quality disentanglement of illumination and appearance in generative 3D gaussian heads. We capture multi-view images of different subjects under various light conditions via lightstage. A dual-branch architecture is employed to separately generate light-invariant gaussian attributes (geometry \mathcal{A}_{geo} and albedo ρ), and physically-based rendering attributes (normal \mathbf{n}_k , roughness σ_k and diffuse light transport coefficients T_k). These attributes together with camera pose and light condition can be splatted into images and compared to the real-world captures to optimize the network.

limit their ability to model the complex interaction between realistic materials and colored illumination. So we propose HeadLighter, a generative model that learns illumination disentanglement from lightstage captures and outputs high-fidelity relightable 3D gaussian heads.

2.2. Portrait Relighting

Portrait relighting [6, 14, 16, 17, 25, 29, 46] aims to render a person’s face under novel lighting conditions. The core challenge lies in solving an ill-posed inverse rendering problem to separate intrinsic properties from the scene’s illumination. [11, 36] capture One-Light-at-a-Time (OLAT) images with Lightstage and render under novel lighting, yielding high-fidelity relighting, but they require controlled capture setting and do not generalize to in-the-wild, sparse-view portraits. To enable relighting a single in-the-wild portrait, subsequent methods introduce various priors and assumptions. Early works [31, 50] rely on strong geometric priors, such as 3D Morphable Models [3]. Others [9, 44, 46] leverage synthetic datasets for training, but face a sim-to-real domain gap. Some works [6, 15] support portrait video relighting which focus on consistency across frames.

More recently, research has shifted towards leveraging the powerful generative priors. Initial attempts treat relighting as a style transfer task within the latent space of 2D GANs [1, 4, 13, 38, 47], but struggled to decouple illumination from other facial attributes like pose and expression. Recently, a growing body of work [12, 18, 24, 26, 28, 33, 34, 41] imposes generative 3D face priors to jointly support relighting and novel-view synthesis. NFL [18] and GSHR [24] enable single portrait relighting through an inversion-then-relight pipeline using self-

supervision. HoloRelight [26] utilizes lightstage data and synthetic data for training which firstly delimits the input and then applies a new lighting condition via an implicit shading representation. 3DPR [34] enables generating a basis of virtual OLAT images from a single portrait and then recombining them for relighting. Our work follows this direction. By integrating a physically-based lighting decomposition into a generative 3D Gaussian framework and training on lightstage data, HeadLighter combines the efficiency of explicit representations, the rich priors of generative models, and the physical accuracy of real-world measurements.

3. Methods

3.1. Preliminaries

3DGS Head GAN leverages neural rendering techniques to learn priors of 3D facial shape and appearance from large-scale 2D image collections. To overcome the computational bottleneck of traditional volumetric rendering, recent works integrate the 3D GAN framework with fast rasterization of 3D Gaussian Splatting (3DGS) [22]. A prominent example is GGHead [23], which employs a StyleGAN2-based generator [20] to map a latent code $z \in \mathbb{R}^{512}$ to multi-channel 2D attribute maps M_* defined in the UV space of a template head mesh. The attributes for 3D Gaussian $\{G_k\}$, can be obtained by sampling the feature maps M_* at UV coordinate x_k^{uv} . These attributes are categorized into: (1) geometric properties, including 3D position $\mu_k \in \mathbb{R}^3$, rotation $\mathbf{q}_k \in \mathbb{R}^4$, scale $\mathbf{s}_k \in \mathbb{R}^3$, and opacity $o_k \in \mathbb{R}$; and (2) view-dependent radiance defined with 1-degree Spherical Harmonics (SH) coefficients $a_k \in \mathbb{R}^{3 \times (1+1)^2}$. The frame-

work is further stabilized with several regularization terms during adversarial training to ensure high-fidelity results.

3.2. Data Acquisition

We capture multi-view One-Light-A-Time using a Light Stage system equipped with 46 calibrated uniform distributed point lights and 28 synchronized cameras. Both the lights and cameras operate at 25 fps. We record under various lighting configurations, including a “**Uniform**” mode with all 46 lights turning on, a “**Direction**” mode where each light is activated together with its neighboring lights, and “**Random**” mode where 10 or 20 lights are randomly selected. To acquire robust 2D detection for dimly lit frames, we insert a fully illuminated frame every 10 frames, assume the subject remains stationary across these 11 frames, and propagate its estimation to the intervening frames. We capture three expressions for each subject: neutral, eyes closed, and smile. We provide more details about the dataset processing in 4.1. The captured images and processed data for participants with authorization will be publicly released.

3.3. Relightable 3DGS Head Generation

We represent a relightable 3D head as a collection of 3D Gaussians $\{g_k\}$, where each Gaussian g_k is associated with a set of geometric and appearance attributes and can be rendered into an image via splatting in a differentiable, physically-based manner, given arbitrary lighting conditions and viewpoints. All attributes of the 3D Gaussians are embedded into structured 2D UV maps of a template head mesh, from which each Gaussian g_k samples its attributes at its assigned UV coordinate. We generate these maps using a dual-branch StyleGAN network that shares the common UV definition and similar network architecture:

- **Base branch** G_{base} predicts the geometric attributes $\mathcal{A}_{\text{geo}} = (\boldsymbol{\mu}_k, \mathbf{s}_k, \mathbf{q}_k, o_k)$ and albedo ρ_k .
- **Relight branch** G_{relit} predicts the relighting-related attributes: surface normal $\mathbf{n}_k \in \mathbb{R}^3$, scalar roughness $\sigma_k \in \mathbb{R}$, and diffuse transport coefficients $\mathbf{T}_k \in \mathbb{R}^{3 \times (s+1)^2}$, where s is the degree of SH coefficients.

Given incident lighting $\mathcal{L} = \{(\omega_i, \mathbf{I}_i)\}_{i=1}^M$, where ω_i denotes the direction of the i -th point light, and $\mathbf{I}_i \in \mathbb{R}^3$ denotes RGB radiance (encoding both color and intensity), the final color c_k of each Gaussian is computed as the sum of diffuse component $c_{\text{diffuse},k}(\mathcal{L})$ and specular component $c_{\text{specular},k}(\mathcal{L}, \omega_o)$, where ω_o is the viewing direction. Then the final color c_k and geometry attributes \mathcal{A}_{geo} of 3D Gaussians can be rendered into images via efficient splatting, enabling high-fidelity, and relightable head synthesis under arbitrary illumination.

Specifically, for the view-independent **diffuse** term $c_{\text{diffuse},k}$, we adopt Precomputed Radiance Transfer (PRT) [39] to model global illumination effects, including

self-occlusion and subsurface scattering. The illumination from each light source is projected into SH coefficient vectors $\mathbf{L}_i \in \mathbb{R}^{(s+1)^2}$. The network predicts per-Gaussian diffuse transport coefficients \mathbf{T}_k , and the diffuse color is calculated by inner products in SH domain, modulated by the albedo ρ_k :

$$c_{\text{diffuse},k}(\mathcal{L}) = \rho_k \odot \sum_{i=1}^M (\mathbf{T}_k \cdot \mathbf{L}_i). \quad (1)$$

The view-dependent **specular** term $c_{\text{specular},k}$ is modeled using a simplified Cook-Torrance microfacet model [10] to create realistic highlights. For improved training stability, we retain only the core Normal Distribution Function (D) while omitting the Fresnel and Geometry terms. The total specular radiance is the sum of contributions from all M light sources:

$$c_{\text{specular},k}(\mathcal{L}, \omega_o) = \sum_{i=1}^M f_{\text{specular}}(\omega_i, \omega_o, \mathbf{n}_k)(\mathbf{n}_k \cdot \omega_i) \mathbf{I}_i, \quad (2)$$

where the specular BRDF f_{specular} is defined as:

$$f_{\text{specular}}(\omega_i, \omega_o, \mathbf{n}_k) = \frac{D(\mathbf{h}_i, \sigma_k)}{4(\mathbf{n}_k \cdot \omega_i)(\mathbf{n}_k \cdot \omega_o)}. \quad (3)$$

Here, $\mathbf{h}_i = \frac{\omega_i + \omega_o}{\|\omega_i + \omega_o\|}$ is the halfway vector for the i -th light source. The D term is modeled by the Trowbridge-Reitz GGX distribution parameterized by the per-Gaussian roughness σ_k :

$$D(\mathbf{h}_i) = \frac{\alpha_k^2}{\pi((\mathbf{n}_k \cdot \mathbf{h}_i)^2(\alpha_k^2 - 1) + 1)^2}, \quad \alpha_k = \sigma_k. \quad (4)$$

3.4. Disentanglement

Our goal is to disentangle intrinsic head appearance and extrinsic illumination in a generative 3D Gaussian head model, supervised by high-fidelity lightstage captures. To achieve stable training, we devise a three-stage training strategy: (1) The first stage trains the base branch G_{base} , adapting a pretrained entangled generator to light-invariant domain. (2) Based on the guidance of the base branch, the second stage trains the relight branch G_{relit} , learning the interaction between incident light and head surfaces using the captured lightstage data. (3) The final stage jointly fine-tunes the entire model to harmonize the predictions from both branches and enhance overall realism.

3.4.1. Stage 1: Base Branch Adaptation

We initialize G_{base} by adapting a pretrained head generative model, GGHead [23]. GGHead does not decouple intrinsic appearance and scene illumination, and its color output – first-order SH coefficients per RGB channel – represents a view-dependent radiance that entangles both factors. We repurpose the pretrained generator to produce a

view-independent RGB albedo map, ρ_k , which represents the intrinsic appearance; while keeping the generator’s internal feature representation unchanged.

The modified generator is first finetuned on the FFHQ dataset using an adversarial loss, which enforces a view-independent radiance, disentangling illumination from the intrinsic appearance at the base level, while preserving generalization ability. Subsequently, it is finetuned for 10k iterations using pseudo albedo maps derived from [18] by adversarial loss. This stage adapts the generator to the domain of albedo (light-invariant), while the short training duration prevents identity collapse.

3.4.2. Stage 2: Relight Priors from LightStage Captures

Stage 2 focuses on training the relight branch G_{relit} , while keeping the base generator G_{base} frozen. We first implement multi-view GAN inversion on G_{base} to obtain geometry and albedo of lightstage captures. We then optimize G_{relit} and latent code per subject to predict relighting-related attributes $(\mathbf{n}_k, \sigma_k, \mathbf{T}_{d,k})$ that match the lightstage observations, where the multi-scale features output by G_{base} are injected into G_{relit} as a guidance. A novel normal distillation and normalization strategy is proposed to enable high-quality normal prediction. We further utilize regularization terms to constrain the generated attributes to be plausible.

Geometry and Albedo Inversion. Given an image sequence captured under varying lighting, we perform multi-view GAN inversion on the fully illuminated frame and propagate the results to the following frames. Specifically, we optimize implicit latent code $\mathbf{w}^+ \in \mathbb{R}^{512 \times L}$ in the extended W^+ space of StyleGAN2 to yield per-Gaussian attributes \mathcal{A}_{geo} and albedo ρ_k , as well as intermediate feature maps $\{\mathbf{F}_{base}^l\}_{l=1}^L$ from G_{base} . We use L2 loss and perceptual loss to constrain the multi-view inversion, and image total variance loss to avoid holes during gaussian rendering:

$$\mathcal{L}_{inv} = \mathcal{L}_2 + \mathcal{L}_{perc} + \mathcal{L}_{tv}. \quad (5)$$

Notably, unlike methods such as PTI [35] that fine-tune the generator weights per subject, our approach keeps the base generator G_{base} fixed throughout inversion to preserve consistent feature representations across different identities in the latent space.

Multi-Scale Feature Guidance. Observing that early layers of G_{base} encode coarse shape (informing global illumination effects), while later layers capture fine details (crucial for normals and roughness), we leverage multi-scale features $\{\mathbf{F}_{base}^l\}_{l=1}^L$ of G_{base} to guide the relight branch. Specifically, a lightweight fusion network Φ^l predicts a residual update Δ^l from the concatenation of the current features of relight branch \mathbf{F}_{relit}^l and the instance-normalized base branch feature \mathbf{F}_{base}^l :

$$\mathbf{F}_{relit}^l = \mathbf{F}_{relit}^l + \Delta^l, \quad \Delta^l = \Phi^l(\mathbf{F}_{base}^l, \mathbf{F}_{relit}^l). \quad (6)$$

This guidance enables G_{relit} to predict relighting attributes consistent with the underlying geometry and albedo from G_{base} while ensuring robust training.

Normal Prediction. Notably, 3DGS does not provide native normals, which are critical for view-dependent specular rendering. One viable method is to extract an explicit mesh from the 3D Gaussian splats and assign nearest face normal to each splat. But mesh extraction for each training iteration is computationally expensive, and the recovered surfaces are sensitive to noise of gaussian splats. An alternative is to use k-NN search to find neighboring splats and compute average orientation as the normal, which is even more susceptible to noise. Since our G_{base} module generates high-quality geometry, its output features $\{\mathbf{F}_{base}^l\}_{l=1}^L$ implicitly contain the geometry information, which could serve as cues for predicting normals. As we have injected the multi-scale base branch feature $\{\mathbf{F}_{base}^l\}_{l=1}^L$ into the relight branch, we propose to directly use G_{relit} to predict the normals, adding 3 channels to its output as the normal map.

To ensure the correctness and smoothness of the predicted normals, we introduce a self-distillation loss and 2D smoothness term. Based on the inverted geometry represented by gaussian point clouds, we pre-extract meshes via poisson reconstruction and cleanup the noise hair region by projecting onto 2D skin-parsing [45] masks. Let $\hat{\mathbf{n}}_{mesh}^k$ be the closest mesh triangle normal of the gaussian splat g_k . We minimize the angular deviation between normalized normal prediction \mathbf{n}_k and $\hat{\mathbf{n}}_{mesh}^k$ via cosine similarity:

$$\mathcal{L}_{normal}^D = \frac{1}{N} \sum_{k=1}^N (1 - \mathbf{n}_k^\top \hat{\mathbf{n}}_{mesh}^k). \quad (7)$$

For the noisy hair region, we utilize a 2D Total Variation loss. We render the normalized normals \mathbf{n}_k as RGB colors of gaussian and splat them to a 2D normal map $I_{norm} \in \mathbb{R}^{H \times W \times 3}$, and apply total variation regularization:

$$\mathcal{L}_{normal}^{TV} = \|\nabla_x I_{norm}\|_1 + \|\nabla_y I_{norm}\|_1, \quad (8)$$

where ∇_x and ∇_y denote horizontal and vertical finite differences.

Training. The final loss of Stage 2 consists of shading loss, the aforementioned normal prediction loss and a regularization term on diffuse transport coefficients T_k . We use these losses to optimize parameters of G_{relit} and a latent code $\mathbf{w}_{lit}^+ \in \mathbb{R}^{512 \times L}$ to represent per-subject head appearance properties.

The shading loss is formulated in Eq. (9), where \mathcal{L}_{tv}^I is involved to prevent image noise.

$$\mathcal{L}_{shading} = \mathcal{L}_{img} + \mathcal{L}_{perc} + \mathcal{L}_{tv}^I. \quad (9)$$

To encourage spectrally smooth diffuse response, we regularize the diffuse transport coefficients $\mathbf{T}_k \in \mathbb{R}^{3 \times 9}$ by

Method	SR	Relit	FID↓	FPS↑
EG3D	✓	×	4.30	42
GGHead	×	×	4.87	228
NFL	✓	✓	4.16	2.8
GSHR	×	✓	5.71	243
Ours	×	✓	4.68	201

Table 1. Comparison of generative quality and rendering speed. **SR** denotes super resolution modules and **Relit** denotes whether to support explicit lighting control. Rendering speed is tested on Nvidia A6000 GPU.

minimizing the variance across the RGB channels:

$$\mathcal{L}_{\text{prt}} = \frac{1}{N} \sum_{k=1}^N \|\mathbf{T}_k - \bar{\mathbf{T}}_k\|_2^2, \quad \bar{\mathbf{T}}_k = \frac{1}{3} \sum_{c \in \{r, g, b\}} \mathbf{T}_k^{(c)}. \quad (10)$$

3.4.3. Stage3: Joint Training

In this final stage, we perform end-to-end training of the full model to further enhance the diversity and realism of generated head images under arbitrary light conditions. We retain the loss functions introduced in Stage 2 to ensure physically plausible relighting outputs from G_{relit} , while additionally incorporating an adversarial loss with a discriminator trained on the FFHQ dataset, to promote high-fidelity and diverse image generation.

In this stage, for adversarial training, we sample random lighting conditions, random base latent code, and random relight latent code, to synthesize albedo, geometry, and relighting-related attributes of a relightable 3DGS head using G_{base} and G_{relit} . Since in Stage 2, the input to G_{relit} is \mathbf{w}^+ code obtained from multi-view inversion. To support random sampling of relight latent code, we first train the mapping network M_{lit} , which maps a randomly sampled latent code $z_{\text{lit}} \in \mathbb{R}^{128}$ into the \mathcal{W}^+ space of G_{relit} , using the optimized $\mathbf{w}_{\text{lit}}^+$ obtained from Stage 2 as training data. To support random sampling of various lighting conditions, we employ an off-the-shelf light estimation method [50] to estimate SH coefficients for FFHQ images.

During each training iteration, we sample random lighting conditions together with random \mathbf{z}^+ (from G_{base}) and $\mathbf{z}_{\text{lit}}^+$ (from M_{lit}) to synthesize a relighted head image. The generated image is then evaluated by a discriminator, which guides the generator toward producing more photo-realistic and diverse outputs. This stage effectively bridges the gap between lightstage captures and in-the-wild images, allowing the model to explore a broader manifold of plausible head appearances under varying illumination.

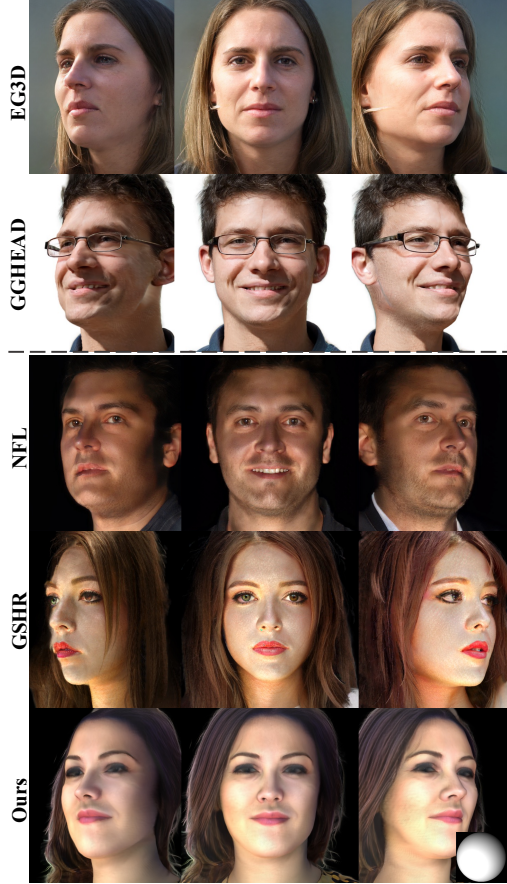


Figure 3. 3D head generation and lighting control. EG3D and GGHEAD do not support explicit lighting control. NFL and GSHR support lighting editing but struggle to handle extreme input lighting (strong, side light), while our method can effectively interact with such challenging conditions. Lighting conditions are provided at the lower right corner.

4. Experiments

4.1. Implementation Details.

Lightstage Dataset. We perform calibration to obtain the world coordinates of each point light and camera. For the captured multi-view images, we use open-source tools to detect 2D landmarks [5] and human segmentation [49] to the "Uniform" frame. All the captured frames are aligned and cropped into 512 resolution. The head pose for each frame is solved using multi-view 2D landmarks and calibrated camera extrinsics, constrained by a 3DMM prior [30]. 56 participants (31 male, 25 female) perform three expressions (neutral, smile, and eyes closed), each recorded under 95 distinct lighting configurations. We select 46 subjects for training and 10 for testing.

Architecture and Training. G_{relit} shares the same overall architecture and number of layers as the G_{base} . However, since G_{base} models complex geometric and textural details

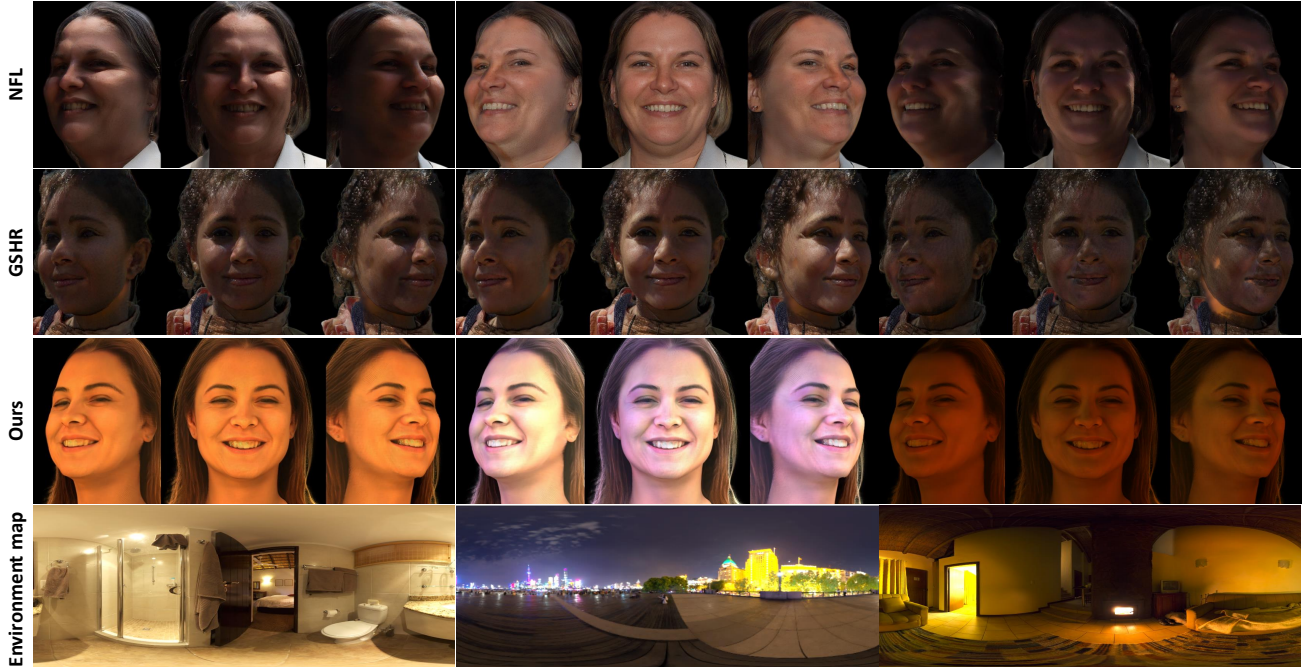


Figure 4. Relighting under complex environment maps. NFL assumes white illumination and fails to handle colored lighting. GSHR lacks real-world OLAT supervision and therefore cannot produce physically plausible responses under complex lighting. In contrast, our method, trained with multi-view OLAT captures, accurately renders realistic shading and reflections under diverse and challenging illumination conditions.

Method	PSNR \uparrow	SSIM \uparrow	LPIPS \downarrow
EG3D	29.29	0.9026	0.065
GGHead	31.53	0.9085	0.052
NFL	30.02	0.9002	0.058
GSHR	30.64	0.8890	0.062
Ours	32.09	0.9132	0.050

Table 2. Evaluation of spatial consistency of generated 3D heads. We render multi-view images from the generated 3D heads and synthesis novel view using NeuS2 [43]; higher PSNR, SSIM, and lower LPIPS indicate better spatial consistency.

that go far beyond face reflectance alone, we design G_{relit} with reduced capacity: the convolutional layers in G_{relit} operate on features of up to 256 dimensions, compared to up to 512 dimensions in G_{base} . Correspondingly, we use a 128-dimensional latent code \mathbf{z}_{lit} to represent face material properties (e.g., albedo, normals, roughness), while geometry and intrinsic appearance are encoded by a 512-dimensional latent code \mathbf{z}_{base} . During Stage 2, G_{relit} is optimized with Adam using a learning rate of 5×10^{-4} , while the lighting latent code \mathbf{w}_{lit} is updated with a higher learning rate of 1×10^{-3} . In Stage 3, both are trained with a reduced learning rate of 1×10^{-4} . Additional details are provided in the supplementary material.

4.2. 3D Generation.

We evaluate generation quality against multiple state-of-the-art 3D-aware head synthesis methods from both qualitative and quantitative perspectives. First, we assess *generation diversity* by generating 50K images and computing FID against the FFHQ dataset [21]. Second, we measure *rendering speed* on one NVIDIA A6000 GPU. Third, we evaluate *multi-view spatial consistency*: for each random latent code, we render 30 viewpoints across -45° to 45° , hold out the frontal view as ground truth to calculate metrics, and use the remaining views to reconstruct the geometry by NeuS2 [43].

As shown in Fig 3, we compare against four state-of-the-art methods: EG3D [8] and NFL [18], which rely on neural volume rendering, and GGHead [23], GSHR [24], which are built upon 3D Gaussian splatting. Among them, EG3D and GGHead do not support explicit illumination control. NFL and GSHR support lighting control, but due to the lack of real-world data, they struggle to respond accurately to complex or extreme lighting conditions. We show the FID score and rendering FPS in Table 1. Methods based on 3D Gaussian achieve significantly higher rendering speeds than volume-rendering counterparts. Our method is slightly slower than GGHead due to the inclusion of a physically-based shading model but maintains the real-time rendering performance. We evaluate multi-view consistency us-

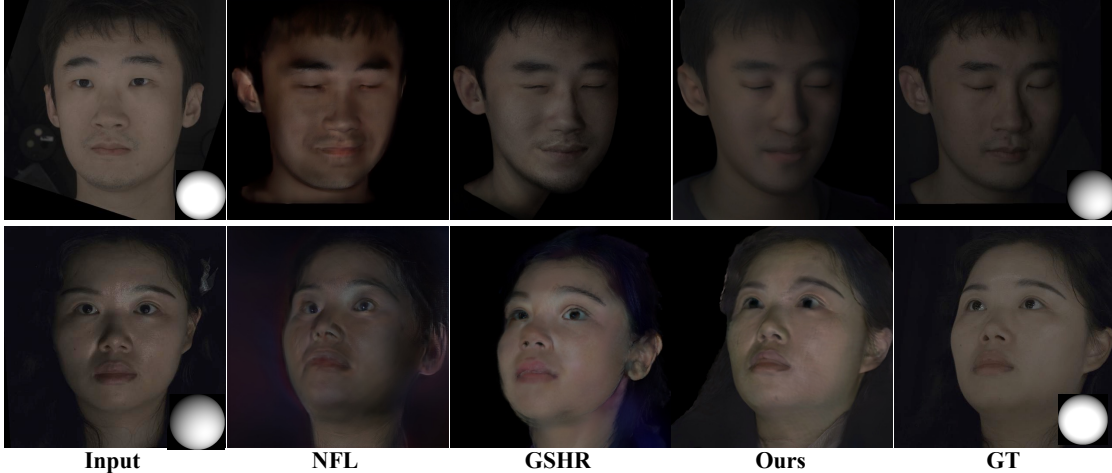


Figure 5. Free view relighting on captured lightstage data. We show the lighting condition at the lower right corner.

Method	PSNR \uparrow	SSIM \uparrow	LPIPS \downarrow
NFL	24.6011	0.8227	0.1179
GSHR	20.0688	0.7464	0.1907
Ours	26.0923	0.8514	0.0988

Table 3. Quantitative comparisons of free view relighting on lightstage captures.

ing a wide viewport range ($\pm 45^\circ$). As shown in Table 3, our method achieves the highest multi-view consistency. Our model is trained on multi-view lightstage face images, which encourages consistency across viewpoints.

4.3. Light Control.

As shown in Figure 4, we compare the lighting control capabilities of different methods. Due to the lack of real-world supervision, NFL achieves disentanglement under a white-light assumption combined with style-mixing, and thus cannot handle colored incident lighting. GSHR is an unsupervised disentanglement method based on 3D Gaussians and it also fails to handle complex or extreme lighting conditions. Our method can handle complex, colored incident lighting with high photorealism. We provide additional comparisons with other methods on lighting control in the supplementary material.

4.4. Portrait Relighting.

We validate the model’s ability to disentangle illumination and appearance using real-captured data. We extract image pairs from lightstage captures and perform free-view relighting using our method and baselines. The first row in the figure shows relighting from uniform illumination to a side-light condition, while the second row demonstrates delighting from non-uniform, dim illumination back to uniform lighting. Compared to baseline methods, our approach

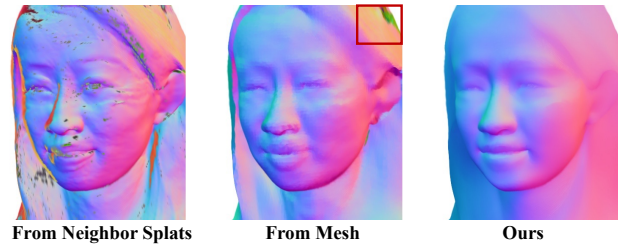


Figure 6. Normal generation with different methods.

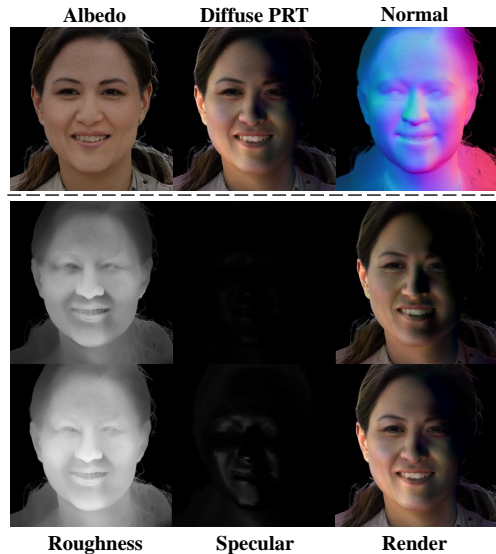


Figure 7. Face Material Editing.

responds more accurately to the input lighting and better preserves the subject’s geometry and appearance. We also provide quantitative results in Tab 3

4.5. Normal Distillation.

We show the normal calculation results of different methods in Fig 6. Directly computing normals from neighboring points in gaussian splats introduces significant noise, making it unsuitable for photorealistic rendering. Reconstructing a mesh from the Gaussian point cloud and then extracting normals is computationally expensive to the training process and often produces noticeable artifacts in fine regions such as hair. To address this, we directly predict normals using the G_{relit} branch, supervised by normals derived from a pre-extracted mesh combined with a 2D total variation loss, yielding smooth and accurate surface normals.

4.6. Face Material Editing.

Thanks to the disentangled representation of intrinsic face materials in our framework, we enable explicit editing of facial appearance properties independent of geometry and illumination. Figure 7 shows a set of results demonstrating control over facial oiliness by adjusting roughness.

5. Conclusion.

We propose a novel framework to disentangle illuminations and intrinsic appearances within a 3D gaussian head generative model supervised by high-fidelity lightstage captures. We utilize a dual-branch architecture to predict geometry with albedo and shading attributes, and employ a progressive training schema to ensure stable training. We further propose a normal supervision method to produce high-quality normals which are crucial for realistic rendering. Experiments demonstrate the generation ability and rendering speed of our method, validate the quality of disentanglement by light and viewport control.

Limitations. The model is static and does not support the control of facial expressions. Furthermore, the number of captured identities and lighting conditions remains limited, which restricts the model’s ability to learn a more comprehensive prior over diverse facial material properties. Future work could address these by incorporating video captures and expanding the dataset scale.

References

- [1] Rameen Abdal, Peihao Zhu, Niloy J Mitra, and Peter Wonka. Styleflow: Attribute-conditioned exploration of stylegan-generated images using conditional continuous normalizing flows. *ACM Transactions on Graphics (ToG)*, 40(3):1–21, 2021. 3
- [2] Florian Barthel, Wieland Morgenstern, Paul Hinzer, Anna Hilsmann, and Peter Eisert. Cgs-gan: 3d consistent gaussian splatting gans for high resolution human head synthesis. *arXiv preprint arXiv:2505.17590*, 2025. 2
- [3] Volker Blanz and Thomas Vetter. A morphable model for the synthesis of 3d faces. In *Seminal Graphics Papers: Pushing the Boundaries, Volume 2*, pages 157–164, 2023. 3
- [4] Mallikarjun BR, Ayush Tewari, Abdallah Dib, Tim Weyrich, Bernd Bickel, Hans-Peter Seidel, Hanspeter Pfister, Wojciech Matusik, Louis Chevallier, Mohamed Elgharib, et al. Photoapp: Photorealistic appearance editing of head portraits. *ACM Transactions on Graphics*, 40(4):1–16, 2021. 3
- [5] Adrian Bulat and Georgios Tzimiropoulos. How far are we from solving the 2d & 3d face alignment problem? (and a dataset of 230,000 3d facial landmarks). In *International Conference on Computer Vision*, 2017. 6
- [6] Ziqi Cai, Kaiwen Jiang, Shu-Yu Chen, Yu-Kun Lai, Hongbo Fu, Boxin Shi, and Lin Gao. Real-time 3d-aware portrait video relighting. In *Proceedings of the IEEE/CVF Conference on Computer Vision and Pattern Recognition*, pages 6221–6231, 2024. 3
- [7] Eric R Chan, Marco Monteiro, Petr Kellnhofer, Jiajun Wu, and Gordon Wetzstein. pi-gan: Periodic implicit generative adversarial networks for 3d-aware image synthesis. In *Proceedings of the IEEE/CVF conference on computer vision and pattern recognition*, pages 5799–5809, 2021. 2
- [8] Eric R Chan, Connor Z Lin, Matthew A Chan, Koki Nagano, Boxiao Pan, Shalini De Mello, Orazio Gallo, Leonidas J Guibas, Jonathan Tremblay, Sameh Khamis, et al. Efficient geometry-aware 3d generative adversarial networks. In *Proceedings of the IEEE/CVF conference on computer vision and pattern recognition*, pages 16123–16133, 2022. 2, 7
- [9] Sumit Chaturvedi, Mengwei Ren, Yannick Hold-Geoffroy, Jingyuan Liu, Julie Dorsey, and Zhixin Shu. Synthlight: Portrait relighting with diffusion model by learning to re-render synthetic faces. In *Proceedings of the Computer Vision and Pattern Recognition Conference*, pages 369–379, 2025. 3
- [10] Robert L Cook and Kenneth E Torrance. A reflectance model for computer graphics. *ACM Siggraph Computer Graphics*, 15(3):307–316, 1981. 4
- [11] Paul Debevec, Tim Hawkins, Chris Tchou, Haarm-Pieter Duiker, Westley Sarokin, and Mark Sagar. Acquiring the reflectance field of a human face. In *Proceedings of the 27th annual conference on Computer graphics and interactive techniques*, pages 145–156, 2000. 3
- [12] Boyang Deng, Yifan Wang, and Gordon Wetzstein. Lumigan: Unconditional generation of relightable 3d human faces. In *2024 International Conference on 3D Vision (3DV)*, pages 302–312. IEEE, 2024. 2, 3, 1
- [13] Yu Deng, Jiaolong Yang, Dong Chen, Fang Wen, and Xin Tong. Disentangled and controllable face image generation via 3d imitative-contrastive learning. In *Proceedings of the IEEE/CVF conference on computer vision and pattern recognition*, pages 5154–5163, 2020. 3
- [14] Yao Feng, Haiwen Feng, Michael J Black, and Timo Bolkart. Learning an animatable detailed 3d face model from in-the-wild images. *ACM Transactions on Graphics (ToG)*, 40(4):1–13, 2021. 3
- [15] Mingtao Guo, Guanyu Xing, and Yanli Liu. High-fidelity relightable monocular portrait animation with lighting-controllable video diffusion model. In *Proceedings of*

- the Computer Vision and Pattern Recognition Conference (CVPR)*, pages 228–238, 2025. 3
- [16] Mingtao Guo, Guanyu Xing, and Yanli Liu. High-fidelity relightable monocular portrait animation with lighting-controllable video diffusion model. In *Proceedings of the Computer Vision and Pattern Recognition Conference*, pages 228–238, 2025. 3
- [17] Andrew Hou, Michel Sarkis, Ning Bi, Yiyong Tong, and Xiaoming Liu. Face relighting with geometrically consistent shadows. In *Proceedings of the IEEE/CVF conference on computer vision and pattern recognition*, pages 4217–4226, 2022. 3
- [18] Kaiwen Jiang, Shu-Yu Chen, Hongbo Fu, and Lin Gao. Nerf-facelighting: Implicit and disentangled face lighting representation leveraging generative prior in neural radiance fields. *ACM Transactions on Graphics*, 42(3):1–18, 2023. 2, 3, 5, 7, 1
- [19] Kaiwen Jiang, Feng-Lin Liu, Shu-Yu Chen, Pengfei Wan, Yuan Zhang, Yu-Kun Lai, Hongbo Fu, and Lin Gao. Nerf-faceshop: learning a photo-realistic 3d-aware generative model of animatable and relightable heads from large-scale in-the-wild videos. *IEEE Transactions on Visualization and Computer Graphics*, 2025. 2
- [20] Tero Karras, Samuli Laine, and Timo Aila. A style-based generator architecture for generative adversarial networks. In *Proceedings of the IEEE/CVF conference on computer vision and pattern recognition*, pages 4401–4410, 2019. 3
- [21] Vahid Kazemi and Josephine Sullivan. One millisecond face alignment with an ensemble of regression trees. In *Proceedings of the IEEE conference on computer vision and pattern recognition*, pages 1867–1874, 2014. 7
- [22] Bernhard Kerbl, Georgios Kopanas, Thomas Leimkühler, and George Drettakis. 3d gaussian splatting for real-time radiance field rendering. *ACM Trans. Graph.*, 42(4):139–1, 2023. 1, 2, 3
- [23] Tobias Kirschstein, Simon Giebenhain, Jiapeng Tang, Markos Georgopoulos, and Matthias Nießner. Gghead: Fast and generalizable 3d gaussian heads. In *SIGGRAPH Asia 2024 Conference Papers*, pages 1–11, 2024. 2, 3, 4, 7
- [24] Henglei Lv, Bailin Deng, Jianzhu Guo, Xiaoqiang Liu, Pengfei Wan, Di Zhang, and Lin Gao. Gsheadrelight: Fast relightability for 3d gaussian head synthesis. In *Proceedings of the Special Interest Group on Computer Graphics and Interactive Techniques Conference Conference Papers*, pages 1–12, 2025. 2, 3, 7
- [25] Yiqun Mei, He Zhang, Xuaner Zhang, Jianming Zhang, Zhixin Shu, Yilin Wang, Zijun Wei, Shi Yan, HyunJoon Jung, and Vishal M Patel. Lightpainter: Interactive portrait relighting with freehand scribble. In *Proceedings of the IEEE/CVF conference on computer vision and pattern recognition*, pages 195–205, 2023. 3
- [26] Yiqun Mei, Yu Zeng, He Zhang, Zhixin Shu, Xuaner Zhang, Sai Bi, Jianming Zhang, HyunJoon Jung, and Vishal M Patel. Holo-relighting: Controllable volumetric portrait relighting from a single image. In *Proceedings of the IEEE/CVF Conference on Computer Vision and Pattern Recognition*, pages 4263–4273, 2024. 3
- [27] Ben Mildenhall, Pratul P Srinivasan, Matthew Tancik, Jonathan T Barron, Ravi Ramamoorthi, and Ren Ng. Nerf: Representing scenes as neural radiance fields for view synthesis. *Communications of the ACM*, 65(1):99–106, 2021. 1
- [28] Xingang Pan, Xudong Xu, Chen Change Loy, Christian Theobalt, and Bo Dai. A shading-guided generative implicit model for shape-accurate 3d-aware image synthesis. *Advances in Neural Information Processing Systems*, 34: 20002–20013, 2021. 2, 3
- [29] Rohit Pandey, Sergio Orts-Escolano, Chloe Legendre, Christian Haene, Sofien Bouaziz, Christoph Rhemann, Paul E Debevec, and Sean Ryan Fanello. Total relighting: learning to relight portraits for background replacement. *ACM Trans. Graph.*, 40(4):43–1, 2021. 3
- [30] Pascal Paysan, Reinhard Knothe, Brian Amberg, Sami Romdhani, and Thomas Vetter. A 3d face model for pose and illumination invariant face recognition. In *2009 sixth IEEE international conference on advanced video and signal based surveillance*, pages 296–301. Ieee, 2009. 6
- [31] Puntawat Ponglertnapakorn, Nontawat Tritrong, and Supasorn Suwajanakorn. Difareli: Diffusion face relighting. In *Proceedings of the IEEE/CVF international conference on computer vision*, pages 22646–22657, 2023. 3
- [32] Anurag Ranjan, Kwang Moo Yi, Jen-Hao Rick Chang, and Oncel Tuzel. Facelit: Neural 3d relightable faces. In *Proceedings of the IEEE/CVF Conference on Computer Vision and Pattern Recognition*, pages 8619–8628, 2023. 2, 1
- [33] Pramod Rao, Gereon Fox, Abhimitra Meka, Mallikarjun BR, Fangneng Zhan, Tim Weyrich, Bernd Bickel, Hanspeter Pfister, Wojciech Matusik, Mohamed Elgharib, et al. Lite2relight: 3d-aware single image portrait relighting. In *ACM SIGGRAPH 2024 Conference Papers*, pages 1–12, 2024. 3
- [34] Pramod Rao, Abhimitra Meka, Xilong Zhou, Gereon Fox, Fangneng Zhan, Tim Weyrich, Bernd Bickel, Hanspeter Pfister, Wojciech Matusik, Thabo Beeler, et al. 3dpr: Single image 3d portrait relight using generative priors. *arXiv preprint arXiv:2510.15846*, 2025. 3
- [35] Daniel Roich, Ron Mokady, Amit H Bermano, and Daniel Cohen-Or. Pivotal tuning for latent-based editing of real images. *ACM Transactions on graphics (TOG)*, 42(1):1–13, 2022. 5
- [36] Shunsuke Saito, Gabriel Schwartz, Tomas Simon, Junxuan Li, and Giljoo Nam. Relightable gaussian codec avatars. In *Proceedings of the IEEE/CVF Conference on Computer Vision and Pattern Recognition*, pages 130–141, 2024. 3
- [37] Katja Schwarz, Yiyi Liao, Michael Niemeyer, and Andreas Geiger. Graf: Generative radiance fields for 3d-aware image synthesis. *Advances in neural information processing systems*, 33:20154–20166, 2020. 2
- [38] Alon Shoshan, Nadav Bhonker, Igor Kviatkovsky, and Gerard Medioni. Gan-control: Explicitly controllable gans. In *Proceedings of the IEEE/CVF international conference on computer vision*, pages 14083–14093, 2021. 3
- [39] Peter-Pike J Sloan, Jan Kautz, and John M Snyder. Precomputed radiance transfer for real-time rendering in dynamic,

- low-frequency lighting environments. *ACM Trans. Graph.*, 2002. 4
- [40] Jingxiang Sun, Xuan Wang, Lizhen Wang, Xiaoyu Li, Yong Zhang, Hongwen Zhang, and Yebin Liu. Next3d: Generative neural texture rasterization for 3d-aware head avatars. In *Proceedings of the IEEE/CVF conference on computer vision and pattern recognition*, pages 20991–21002, 2023. 2
- [41] Feitong Tan, Sean Fanello, Abhimitra Meka, Sergio Orts-Escolano, Danhang Tang, Rohit Pandey, Jonathan Taylor, Ping Tan, and Yinda Zhang. Volux-gan: A generative model for 3d face synthesis with hdri relighting. In *ACM SIGGRAPH 2022 Conference Proceedings*, pages 1–9, 2022. 2, 3
- [42] Junshu Tang, Bo Zhang, Binxin Yang, Ting Zhang, Dong Chen, Lizhuang Ma, and Fang Wen. 3dfaceshop: Explicitly controllable 3d-aware portrait generation. *IEEE transactions on visualization and computer graphics*, 30(9):6020–6037, 2023. 2
- [43] Yiming Wang, Qin Han, Marc Habermann, Kostas Daniilidis, Christian Theobalt, and Lingjie Liu. Neus2: Fast learning of neural implicit surfaces for multi-view reconstruction. In *Proceedings of the IEEE/CVF International Conference on Computer Vision*, pages 3295–3306, 2023. 7
- [44] Zhibo Wang, Xin Yu, Ming Lu, Quan Wang, Chen Qian, and Feng Xu. Single image portrait relighting via explicit multiple reflectance channel modeling. *ACM Transactions on Graphics (ToG)*, 39(6):1–13, 2020. 3
- [45] Valikhujaev Yakhyokhuja. face-parsing. <https://github.com/yakhyo/face-parsing>, 2024. GitHub repository. 5
- [46] Yu-Ying Yeh, Koki Nagano, Sameh Khamis, Jan Kautz, Ming-Yu Liu, and Ting-Chun Wang. Learning to relight portrait images via a virtual light stage and synthetic-to-real adaptation. *ACM Transactions on Graphics (TOG)*, 41(6):1–21, 2022. 3
- [47] Ran Yi, Teng Hu, Mengfei Xia, Yizhe Tang, and Yong-Jin Liu. Feditnet++: Few-shot editing of latent semantics in gan spaces with correlated attribute disentanglement. *IEEE Transactions on Pattern Analysis and Machine Intelligence*, 2024. 3
- [48] Zhengming Yu, Tianye Li, Jingxiang Sun, Omer Shapira, Seonwook Park, Michael Stengel, Matthew Chan, Xin Li, Wenping Wang, Koki Nagano, and Shalini De Mello. GAIA: Generative animatable interactive avatars with expression-conditioned gaussians. In *ACM SIGGRAPH*, 2025. 2
- [49] Peng Zheng, Dehong Gao, Deng-Ping Fan, Li Liu, Jorma Laaksonen, Wanli Ouyang, and Nicu Sebe. Bilateral reference for high-resolution dichotomous image segmentation. *arXiv preprint arXiv:2401.03407*, 2024. 6
- [50] Hao Zhou, Sunil Hadap, Kalyan Sunkavalli, and David W Jacobs. Deep single-image portrait relighting. In *Proceedings of the IEEE/CVF international conference on computer vision*, pages 7194–7202, 2019. 3, 6

HeadLighter: Disentangling Illumination in Generative 3D Gaussian Heads via Lightstage Captures

Supplementary Material

6. Implementation Details

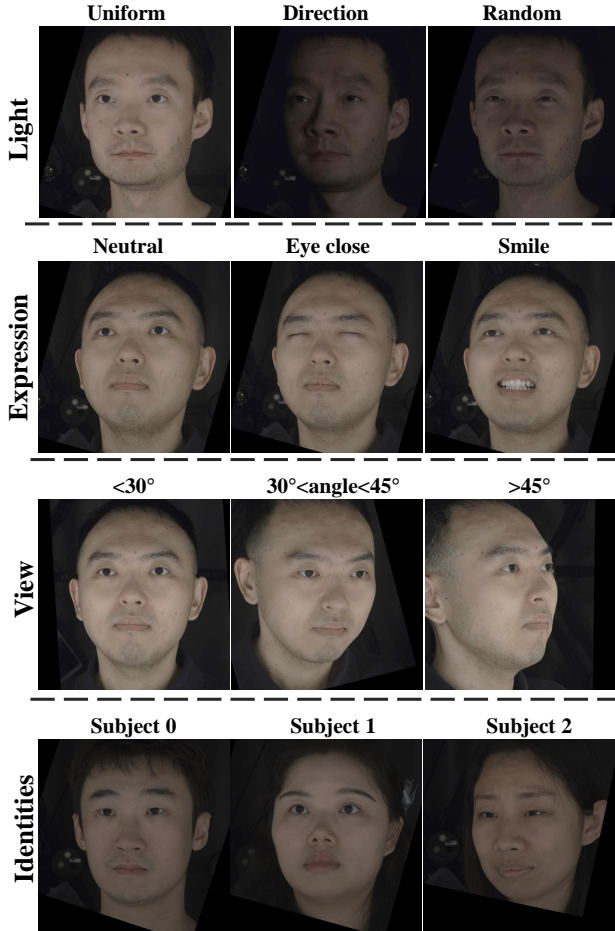


Figure 8. An overview of the lightstage captures.

Dataset. We provide a summarized overview of the LightStage dataset in Fig 8. The dataset encompasses diverse subjects, lighting conditions, facial expressions, and viewing angles. The lighting conditions are categorized into three types: uniform, directional, and random. The facial expressions include neutral, smiling, and closed eyes.

Training. We provide hyper parameters and configurations of training in this section.

- **Stage1:** We retain the majority of the pretrained GGHead model’s architecture and parameters, and modify only the final layer to output RGB values instead of the original spherical harmonic coefficients. We fine-tune this modi-

fied model for 80,000 iterations on the FFHQ dataset using an adversarial loss. We then generate 10,000 pseudo-albedo images using NFL [18]. To prevent identity collapse, we use a large truncated ψ value, which controls the diversity of sampled latent codes by constraining the sampling region in the latent space. We fine-tune the model for an additional 10,000 iterations on these pseudo-albedo images with an adversarial loss, removing the lighting component from the pretrained GGHead model while maintaining the diversity of the generated identities.

- **Stage2-Inversion:** We achieve multi-view inversion under the supervision of multiple loss terms. We set the weight of the \mathcal{L}_2 to 0.1, the weight of the \mathcal{L}_{perc} to 1, and the weight of \mathcal{L}_{tv} to 0.01. We compute the perceptual loss only using frontal images. The inversion process requires 500 iterations, and the inversion result of the previous fully lit frame serves as the initial value for the next frame to accelerate convergence.
- **Stage2-Network:** We employ a lightweight network including 2 layers and Leaky ReLU activation to enable multi-scale features of G_{base} to guide the relight branch. We design G_{relit} with a reduced feature dimensionality: its convolutional layers operate on 256-dimensional features, compared to 512 in G_{base} . Finally, the relight branch requires approximately 90 MB memory storage.
- **Stage2-Training:** We set weights of \mathcal{L}_{normal}^D , $\mathcal{L}_{normal}^{TV}$ to be 1 and 10 respectively. The weights of \mathcal{L}_{img} , \mathcal{L}_{perc} and \mathcal{L}_{tv}^I are 1. And weight of \mathcal{L}_{prt} is set to 0.5.
- **Stage3-Training:** Firstly, we train mapping network M_{lit} for 10k iterations. Then we train the two branches using losses mentioned in Stage 2 and additional adversarial loss. The parameters of discriminator are fixed.

7. More Comparisons

We also provide comparisons with FaceLit [32] in Fig 10 and LumiGAN [12] in Fig 9. Both FaceLit and LumiGAN are unsupervised disentanglement methods based on volume rendering, which struggle with extreme lighting conditions and often produce unrealistic lighting artifacts. Moreover, FaceLit relies on a white-light assumption and therefore cannot handle colored lighting. In contrast, our method supports diverse lighting inputs, including color environment maps, point lights, and spherical harmonic coefficients. It also produces natural lighting and shadow effects even under strong side lighting conditions.



Figure 9. Comparisons with LumiGAN [12].

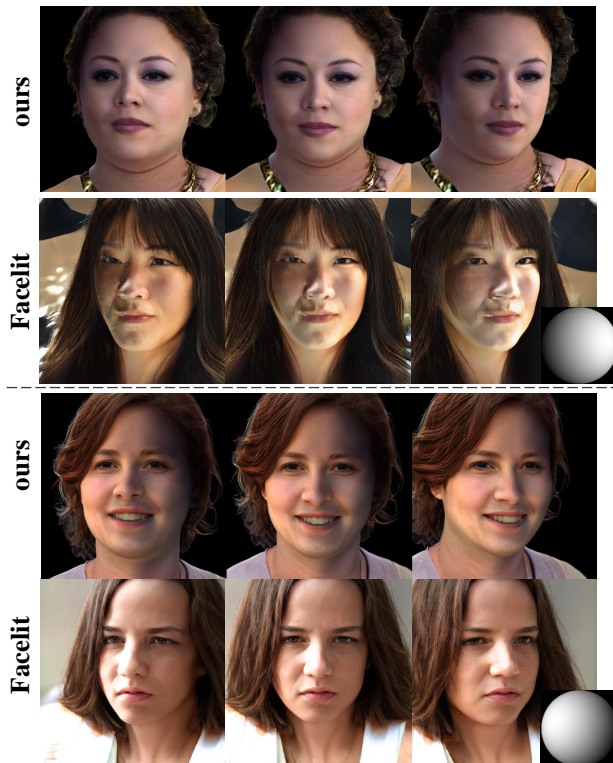


Figure 10. Comparisons with FaceLit [32].

9. Ethical Considerations

The generation of artificial portrait using our method poses risks, including the spread of false information, and erosion of trust in media credibility. These issues could have profound societal implications. Addressing this challenge requires developing reliable techniques to identify and verify authentic content.

8. Generation Results.

Fig 11 shows additional identities generated under various lighting conditions. Our method produces diverse facial materials and supports relighting under low-light environments and multiple environmental maps.



Figure 11. **More Generation Results.** We show the corresponding environment maps at the right down corner.